Hindawi
Science and Technology of Nuclear Installations
Volume 2018, Article ID 5094810, 13 pages
https://doi.org/10.1155/2018/5094810

Research Article

Experimental and Numerical Studies on Sloshing Dynamics of PCS Water Tank of Nuclear Island Building

Xiaojun Li[1,2] **Chenning Song**[1] **Guoliang Zhou**[3] **Chao Wei**[3] **and Ming Lu**[4]

[1] *The College of Architecture and Civil Engineering, Beijing University of Technology, Beijing 100124, China*
[2] *Institute of Geophysics, China Earthquake Administration, Beijing 100081, China*
[3] *Nuclear and Radiation Safety Center, Ministry of Environmental Protection of the People's Republic of China, Beijing 100082, China*
[4] *Institute of Crustal Dynamics, China Earthquake Administration, Beijing 100085, China*

Correspondence should be addressed to Chenning Song; scanner2007@163.com

Received 30 November 2017; Revised 25 March 2018; Accepted 4 April 2018; Published 20 May 2018

Academic Editor: Michel Giot

Water tank is one important component of passive containment cooling system (PCS) of nuclear island building. The sloshing frequency of water is much less than structure frequency and large-amplitude sloshing occurs easily when subjected to seismic loadings. Therefore, the sloshing dynamics and fluid-structure interaction (FSI) effect of water tank should be considered when the dynamic response of nuclear island building is analyzed. A 1/16 scaled model was designed and the shaking table test was done, in which the hydrodynamic pressure time histories and attenuation data of wave height were recorded. Then the sloshing frequencies and 1st sloshing damping ratio were recognized. Moreover, modal analysis and time history analysis of numerical model were done by ADINA software. By comparing the sloshing frequencies and hydrodynamic pressures, it is proved that the test method is reasonable and the formulation of potential-based fluid elements (PBFE) can be used to simulate FSI effect of nuclear island building.

1. Introduction

Passive containment cooling system (PCS) is the significant characteristic of the third-generation nuclear power plants [1], which is different from the traditional nuclear power plants. It is known that the sloshing frequency of water is far less than structure frequency, so the long period components of seismic loadings could not be ignored in the analysis of water tank. Moreover, the influence of water tank on floor response spectra under seismic loadings should be considered emphatically. The dynamic characteristics of water tank should be studied to analyze the seismic response of nuclear island building accurately.

FSI effect is the key problem for dynamic analysis of water tank of nuclear island building. Related to the type of external loads, shape of container, and depth of liquid, the motion of free fluid surface may be simple planar, nonplanar, breaking, and so on [2–4]. Focused on the nonlinear sloshing in a rectangular tank, Faltinsen et al. [5, 6] studied the horizontal, vertical, and pitching motion. Moreover, the stable and unstable frequency domains of the planar resonant standing waves, the swirling waves, and the square-like resonant standing waves were researched. In the research on FSI effect of nuclear power plants, Lo Frano and Forasassi [7–9] did some research on liquid metal nuclear reactor considering the FSI effect subjected to seismic loads. Zhao et al. [10] used the Arbitrary Lagrange Eulerian (ALE) algorithm to simulate the seismic response of AP1000 shield building and studied the influence of water tank. The research showed that water tank could reduce the dynamic response of structure. Xu et al. [11] used the smoothed particle hydrodynamics (SPH) and finite element method (FEM) coupling method to simulate the FSI. The research showed that the water tank could decrease the natural frequency and response of the shield building. Lu et al. [12] built a scaled elevated tank to investigate the seismic response of shield building under transient loadings. Moreover, numerical models were established and the numerical results of acceleration and

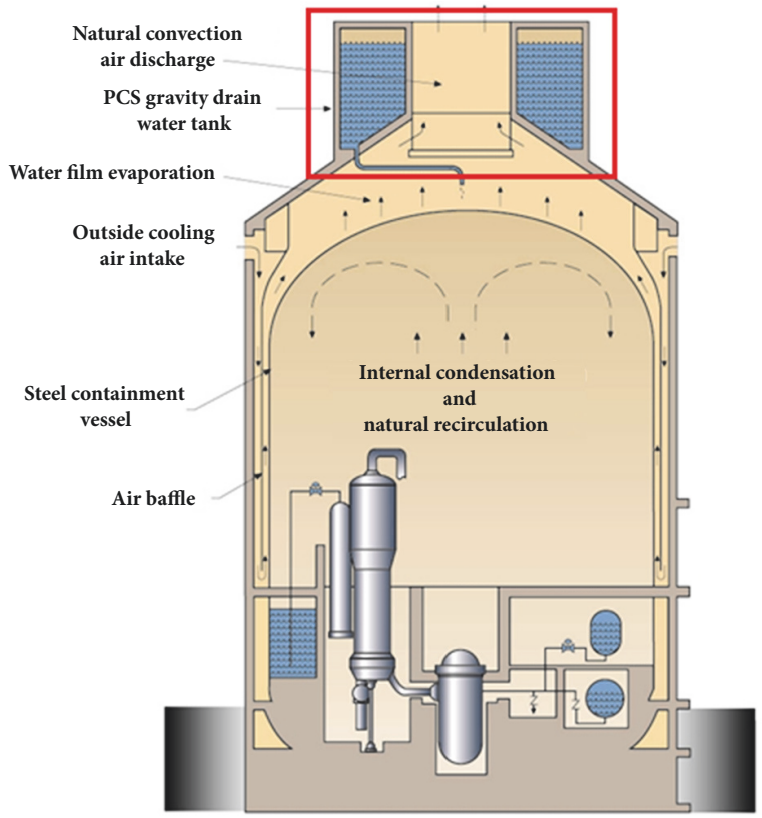

Figure 1: PCS of nuclear island building [20].

displacement were in good agreement with the experiment. Liu et al. [13] did the shaking table test of a scaled elevated tank of passive containment cooling system water storage tank (PCCWST). An equivalent mechanical model was used to predict the seismic forces of the PCCWST subjected to horizontal ground excitation and the numerical results had a good agreement with the experiment.

In the research on dynamic characteristics of water tank, the main test method is using laser displacement sensor to measure the sloshing displacement of water; then the sloshing frequency could be calculated [14]. Aimed at sloshing damping ratio, the analytical solution or approximate solution was derived only for containers with regular shape. The dynamic experiment was the commonly used method to obtain sloshing damping ratio, but the experimental results lacked repeatability because of the nonlinear characteristic.

Sloshing frequency and damping ratio are the key parameters of dynamic characteristic of the water tank. Moreover, they are also the key parameters to simplify the sloshing analysis based on Housner model. Related scholars have done some research on the sloshing frequency [15–17] and specifications [18, 19] and also give the simplified calculation formulas on regular cylindrical tanks. But, for irregular annular cylindrical water tank, related specifications do not give detailed introduction. Aimed at sloshing damping ratio, suggested values have been given for regular containers, but, for irregular containers, the research and verification are deficient. As shown in Figure 1, PCS water tank is one kind of irregular annular cylindrical water tank and the suggestion of relevant parameter may not be available in this case.

This study focuses on the interaction effects between the tank and water for the water tank of nuclear island building. As for the interaction effects between the water tank and nuclear island building, it will be studied separately. In this study, a 1/16 scaled model was made for shaking table test. Pore water pressure sensors (PWPS) were arranged along the different height of tank walls and the cameras were arranged on the top of the tank, and the hydrodynamic pressure time-histories and attenuation data of wave height were collected. The sloshing frequencies and 1st sloshing damping ratio can be obtained based on the test data. By comparing the experimental and numerical analysis results, the reasonableness of experimental method and the accuracy of numerical method are verified.

2. Shaking Table Test

2.1. Introduction of Model. Similarity relation of the experimental model was shown in Table 1. In this test, geometry L, elastic modulus E, and density ρ were chosen as the basic similar constants. According to the size of shaking table, the materials of model, the fluid characteristic, and the feasibility of test, the similarity rules S_l, S_E, and S_ρ were equal to 1/16, 1/3, and 1. Then other similarity rules could be calculated.

Table 1: Similarity relation of the experimental model.

Physical quantity	Similarity rule	Similarity parameter
Geometry L	S_l	1/16
Elastic modulus of concrete E_C	S_E	1/3
Density of concrete ρ_C	S_{ρ_c}	1
Bulk modulus of liquid G_L	S_G	1
Density of liquid ρ_L	S_{ρ_l}	1
Time *of* input motion t	S_t	0.108
Amplitude of input motion a	S_a	5.333

(a)

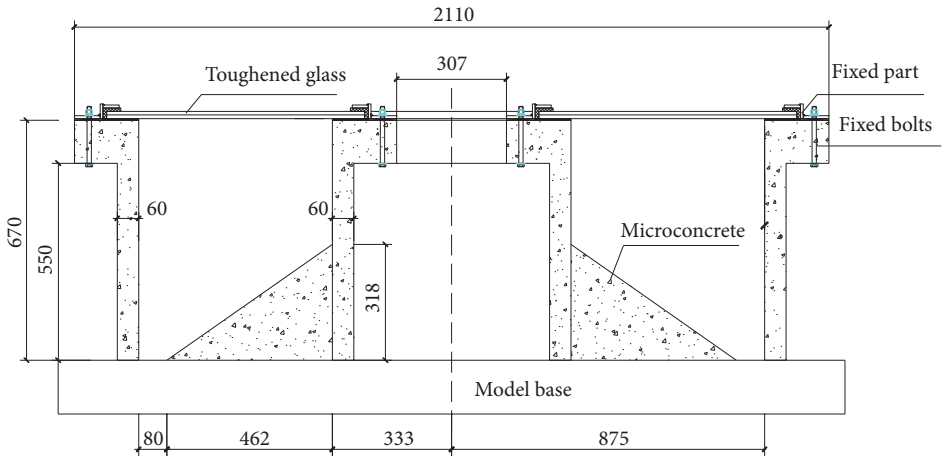

(b)

Figure 2: Introduction of model (unit : mm). (a) Experimental model. (b) The profile and geometry sizes.

To satisfy the rigid assumption of water tank, the tank walls and bottom were made using microconcrete and the steel bars were replaced by galvanized iron wires. To test the wave height, the roof of water tank was replaced by toughened glass and connected to the water tank with fixed parts. The experimental model and the geometry sizes are shown in Figure 2.

To study the sloshing characteristic of liquid, the existing test instruments are often laser displacement sensor or laser vibration measuring instrument. Common laser displacement sensor might not satisfy the testing precision, but the high precision instruments or collection systems are very expensive. According to the theory of laser measurement, colored substance dissolved by organic solvent is used to increase laser reflection. However, organic solvent like lacquer thinner is easily volatile and may bring some risks. Moreover, this method could not catch the splash liquid during the test [12] and the organic solvent may change the sloshing characteristic of liquid itself. Therefore, to recognize the sloshing frequencies, PWPS shown in Figure 3 was used to measure the hydrodynamic pressure in this paper.

To record the hydrodynamic pressure data, sixteen PWPS were divided into two groups and they were arranged along the height of tank walls in x cross section and y cross section separately. To record the attenuation data of wave height, rulers were arranged at the tank walls in x cross section and y cross section. In addition, cameras were arranged on the top of toughened glass. The PWPS can be placed in water

Table 2: Material parameters of experimental model.

Material parameters	Microconcrete	Toughened glass	Galvanized iron wires	Water
Density (kg/m^3)	2350	2560	7800	1000
Young's modulus (Pa)	1.05×10^{10}	7.20×10^{10}	2.06×10^{11}	—
Bulk modulus (Pa)	—	—	—	2.30×10^{9}
Poisson's ratio	0.17	0.20	0.30	—

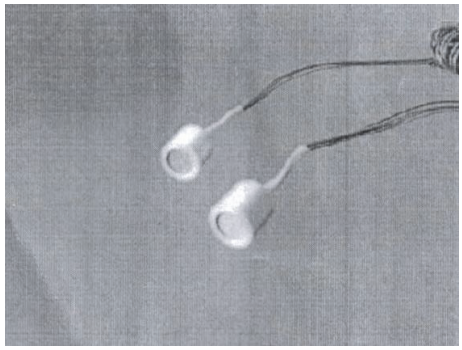

Figure 3: Pore water pressure sensors (PWPS).

to record water pressures, the measurement ranges of PWPS are 30 kPa or 50 kPa, the strain output of full range is about 500×10^{-6}, and the precision of sensors is 0.3% F·S. The arrangements of PWPS and cameras are shown in Figure 4. The material parameters of experimental model are listed in Table 2.

2.2. Experiment Process. According to the geometrical scale of 1/16, the height of free water surface is 550 mm. To recognize the sloshing frequencies, single-direction sine waves were used. The normalized sine wave is shown in Figure 5(a) and the peak ground acceleration is 0.05 g and 0.10 g. To verify the reasonableness of numerical results, the three-direction acceleration time histories were used as inputs. Considering the space limit, one set of inputs is shown in this paper. The time history curves are shown in Figure 5(b) and the peak ground acceleration of three-direction time histories is 1.20 g, 0.80 g, and 0.60 g separately. Hydrodynamic pressure and attenuation data of wave height were recorded. Then the sloshing frequencies and 1st sloshing damping ratio were obtained.

2.3. Data Analysis

2.3.1. Recognition of Sloshing Frequency. FFT is widely used in the field of physics, acoustic, optics, structure dynamics, and signal processing. Based on FFT of data-signal, the sloshing frequency of liquid can be recognized through hydrodynamic pressure. The typical application of FFT is changing time histories into amplitude-frequency curves and the basic equation is shown as follows:

$$F(\omega) = \int_{-\infty}^{+\infty} f(t)\, e^{-i\omega t} dt, \tag{1}$$

where $f(t)$ is the time history of data-signal, $F(\omega)$ is the spectrum function of $f(t)$, and ω is the frequency.

In the experiment, the liquid would keep sloshing and the wave height would gradually decay after the external excitation is ended. At that time, the hydrodynamic pressure and wave height only reflect the dynamic characteristic of liquid in the tank without external excitation. As shown in Figure 6, hydrodynamic pressure in the free sloshing range was got and the pressure time curves could be changed into amplitude-frequency curves by FFT. From Figure 6(c), the sloshing frequencies can be recognized.

Low sloshing frequencies play a control action in the dynamic analysis of liquid and seismic design of containers, especially the 1st sloshing frequency. So the first few sloshing frequencies are needed to be recognized. The statistical results of first four sloshing frequencies recognized by hydrodynamic pressure data are listed in Table 3. Moreover, forty samples are chosen and the errors between average value and test value are shown in Figure 7.

As shown in Table 3, the coefficients of variation are all less than 5%. In Figure 7, the maximum errors of first four sloshing frequencies are 3.56%, 5.96%, 5.68%, and 2.91% separately. It proves that the test values have little discreteness and the results are acceptable.

2.3.2. Recognition of 1st Sloshing Damping Ratio. As one important dynamic parameter, sloshing damping is mainly from the friction between liquid and container. The value is related to four factors: viscous damping of inner wall, viscous dissipation of free fluid surface, viscous dissipation of liquid inside, and capillary of liquid inside. The sloshing damping ratio is often obtained through experiment because of the complexity of parameters. In this study, the 1st natural frequency of water tank is more than 50 Hz and the model could be regarded as rigid tank. The specifications propose that the basic sloshing damping ratio is 0.5% for normal tanks. However, it should be noted that, for higher viscosity fluids and tanks with internal baffles, the damping ratio is higher. For the impulsive components, the basic damping ratio is generally assumed to be approximately 2%. For irregular containers, the specification does not give the suggestion.

Logarithmic decrement method is often used to calculate the damping ratio of structure and the equation is shown:

$$\delta = \ln \frac{\mu_i}{\mu_{i+1}} = \frac{2\pi\xi}{\sqrt{1-\xi^2}}, \tag{2}$$

where δ is the logarithmic decrement, μ_i and μ_{i+1} are the amplitudes of two adjacent periods, and ξ is the damping ratio.

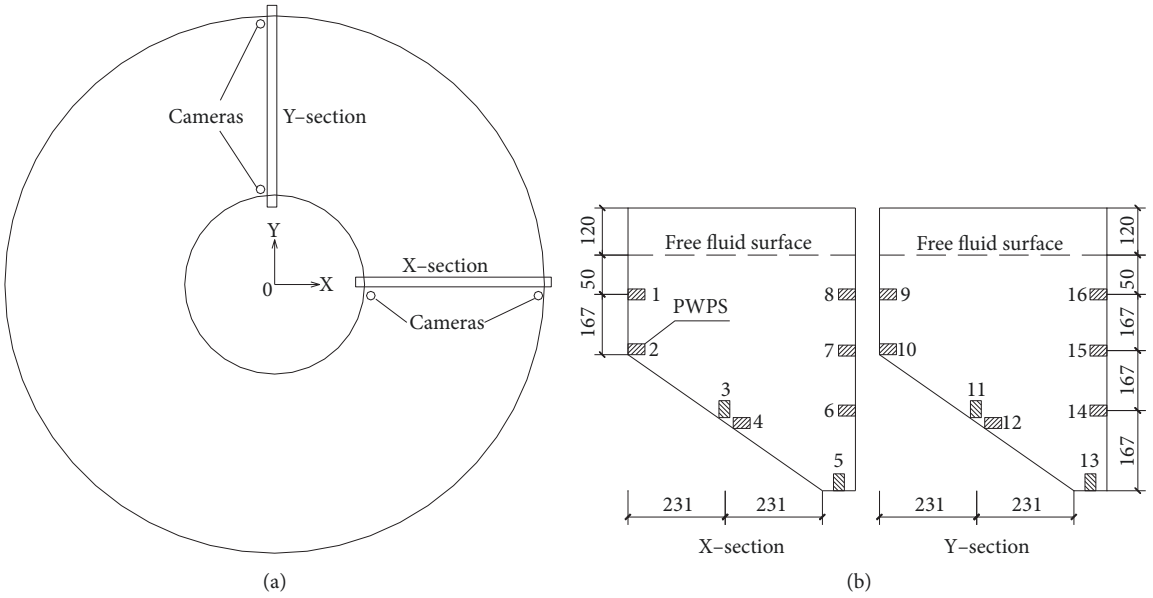

FIGURE 4: Layout of instruments. (a) Top view of model. (b) Layout of PWPS.

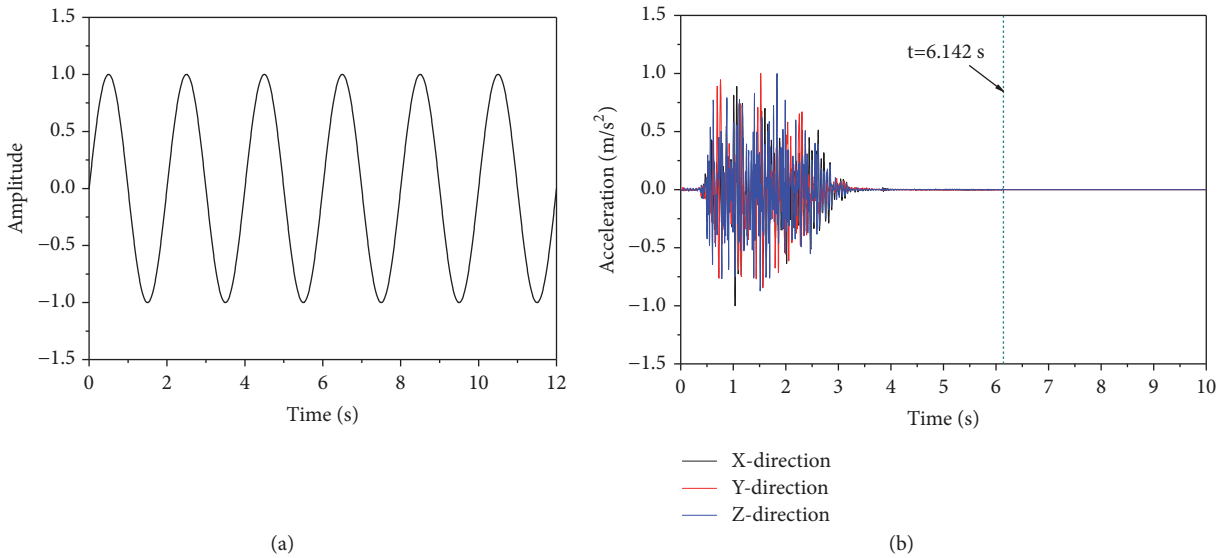

FIGURE 5: Input time history curves for shaking table test. (a) Normalized sine wave. (b) Normalized seismic inputs in three directions.

On account of the small sloshing damping, the free vibration of liquid decays slowly. To satisfy the accuracy requirement, the amplitudes of j adjacent periods are used to calculate the damping ratio. The damping ratio of small damping system can be calculated using the following equation:

$$\xi \approx \frac{1}{2\pi j} \ln \frac{\mu_i}{\mu_{i+j}}. \tag{3}$$

Logarithmic decrement method is one of the main methods to calculate the damping ratio. Although (2) and (3) are derived by SDOF system, they are also applicable for MDOF [21]. The basic modal damping ratio (1st damping ratio) can be obtained easily by free vibration test. The key to measure higher modal damping ratio is to motivate free vibration of the corresponding mode. To FSI system, it is reasonable to consider the structure and the fluid, respectively [21]. The attenuation data of wave height are the parameters of sloshing water and logarithmic decrement method can be used in this paper.

As shown in Table 3, the 1st sloshing frequency is about 0.5 Hz. The period of sine wave input shown in Figure 5(a) is 2.0 s, so the 1st vibration mode can be motivated and the 1st sloshing damping ratio can be calculated. Based on (3), The records from cameras are chosen to calculate 1st sloshing damping ratio of water. The results are shown in Table 4 and Figure 8.

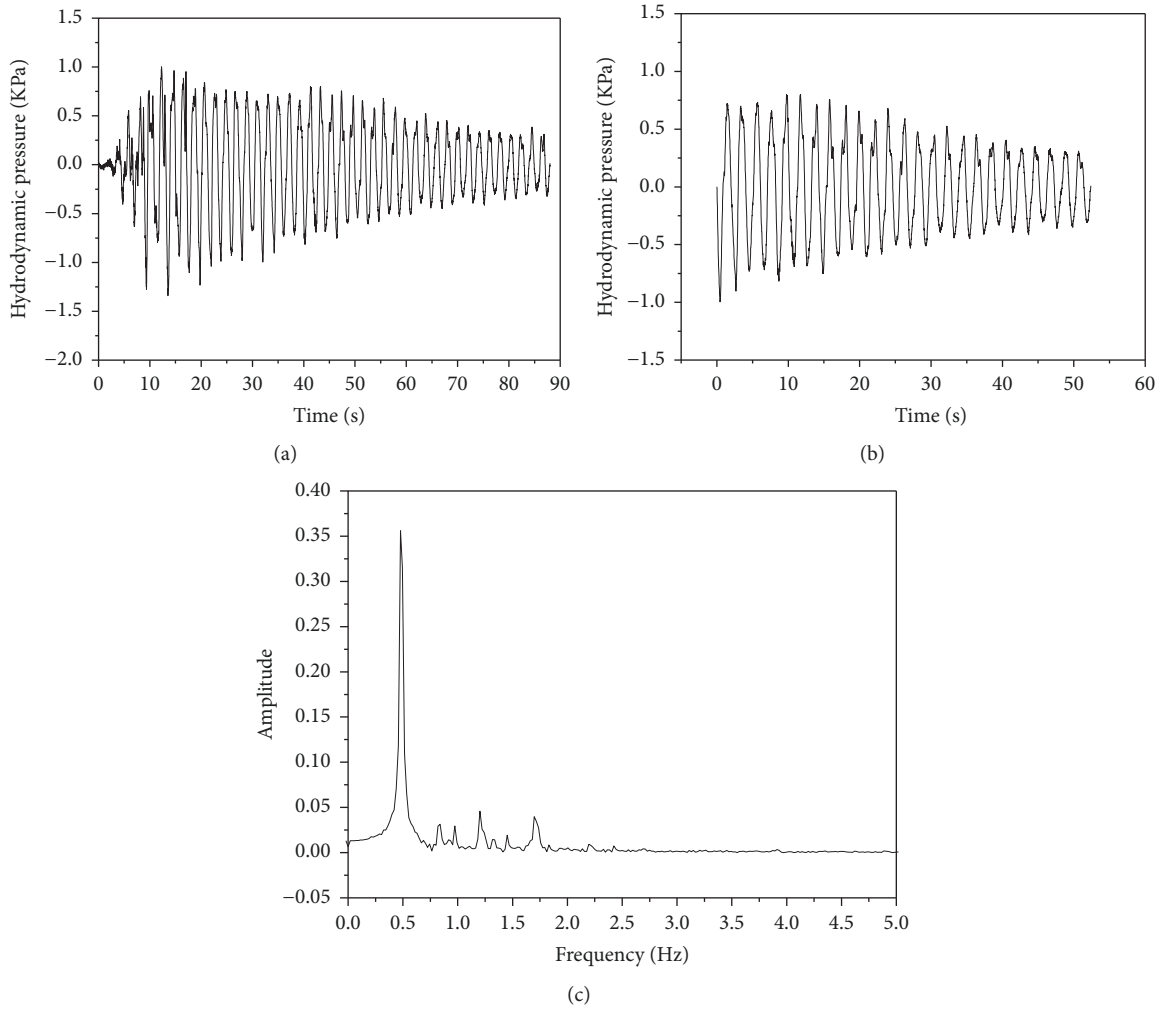

Figure 6: Data processing of hydrodynamic pressure records at No. 8 PWPS. (a) Time history curve. (b) Free sloshing range. (c) Amplitude-frequency curve.

Table 3: First four sloshing frequencies.

Modes	Average value (AVG) (Hz)	Standard deviation (SD) (Hz)	Coefficient of variation (%)
1	0.4938	0.0090	1.82
2	0.8404	0.0270	3.21
3	1.0015	0.0267	2.67
4	1.2188	0.0194	1.59

As shown in Table 4, The coefficient of variation is less than 5% and the discreteness is small. In Figure 8, the test values are almost between AVG − SD and AVG + SD. It proves that the experimental results are reasonable and reliable. The average value of 1st sloshing damping ratio is 0.5138% and it does not have much difference with the suggestion for the regular water tank in the specifications. Although the bottom of PCS water tank is inclined and the shape is irregular, 1st sloshing damping ratio changes little. The reasons may be that the water tank is not irregular especially and the sloshing damping ratio is too small. As a supplement, this conclusion may not be available for other irregular water tanks.

3. Numerical Analysis and Discussion

3.1. Description of Numerical Model. In the field of FSI, ADINA software has strong solving capability. The equations of the $\phi - u$ formulation in this study are briefly introduced in this part.

As the special fluid element in ADINA [22], the potential-based fluid elements (PBFE) can be used for frequency and time history analyses of structure [23, 24]. The basic assumptions are that the fluid is inviscid, compressible, or incompressible, with irrotational motion and small amplitude. There are two basic parameters in the formulation:

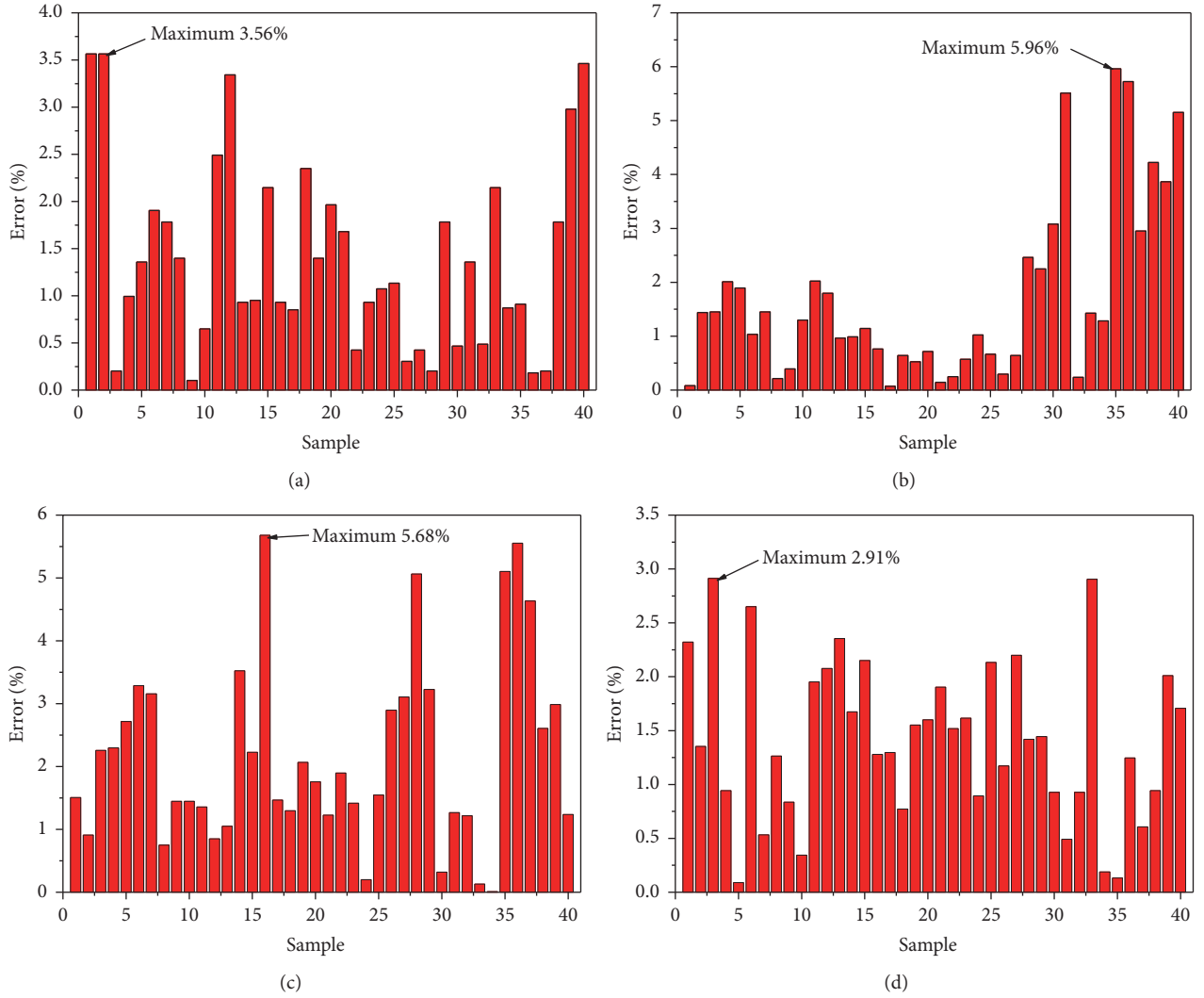

Figure 7: Statistics of errors between average value and test value. (a) 1st sloshing frequency. (b) 2nd sloshing frequency. (c) 3rd sloshing frequency. (d) 4th sloshing frequency.

Table 4: Statistics of 1st sloshing damping ratio.

Average value (AVG) (%)	Standard deviation (SD) (%)	Coefficient of variation (%)
0.5138	0.0212	4.13

velocity potential in fluid domain ϕ and displacement in solid domain u. The velocity potential ϕ satisfies the wave equation:

$$\nabla^2\phi = \frac{1}{C_w^2}\frac{\partial^2\phi}{\partial^2 t}, \tag{4}$$

where ∇^2 is the Laplace differential operator, t is the time variable, and C_w is the wave velocity in fluid which is given by

$$C_w = \sqrt{\frac{\kappa_w}{\rho_w}}, \tag{5}$$

where ρ_w is water density and κ_w is the bulk modulus. Based on the standard theories, the variational form of (4) can be got as

$$\frac{\rho_w}{C_w^2}\int_{V_w}\frac{\partial^2\phi}{\partial t^2}\delta\phi\, dV + \rho_w\int_{S_w}\dot{\mathbf{u}}\cdot\mathbf{n}\delta\phi\, dS + \rho_w\int_{V_w}\nabla\phi \cdot \delta\nabla\phi\, dV = 0, \tag{6}$$

where V_w is the volume of water and S_w is water boundary where normal velocity is prescribed. Under earthquake, the dynamic response of the water tank is coupled through compatibility of velocity potential and prescribed normal

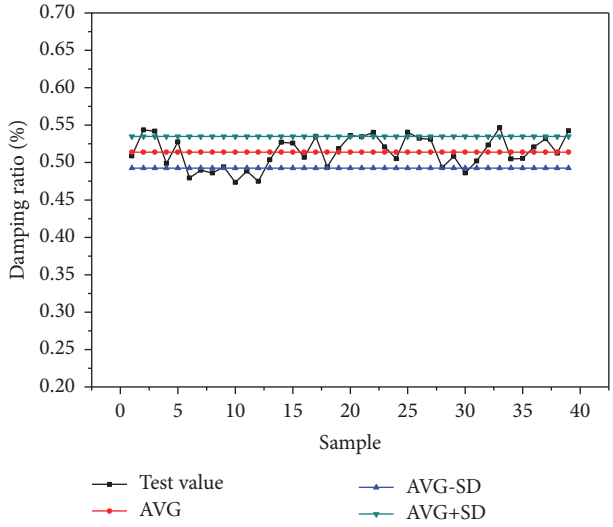

Figure 8: Statistics of 1st sloshing damping ratio.

velocity at the fluid-structure interface. The system dynamic equations of the tank filled with water can be obtained [25]:

$$\begin{bmatrix} \mathbf{M}_{ss} & 0 \\ 0 & -\mathbf{M}_{ww} \end{bmatrix} \begin{bmatrix} \ddot{\mathbf{U}} \\ \ddot{\mathbf{\Phi}} \end{bmatrix} + \begin{bmatrix} \mathbf{C}_{ss} & \mathbf{C}_{sw} \\ \mathbf{C}_{ws} & 0 \end{bmatrix} \begin{bmatrix} \dot{\mathbf{U}} \\ \dot{\mathbf{\Phi}} \end{bmatrix} + \begin{bmatrix} \mathbf{K}_{ss} & 0 \\ 0 & -\mathbf{K}_{ww} \end{bmatrix} \begin{bmatrix} \mathbf{U} \\ \mathbf{\Phi} \end{bmatrix} = \begin{bmatrix} -\mathbf{M}_{ss}\mathbf{1}\ddot{u}_g(t) \\ -\mathbf{C}_{ws}\mathbf{1}\dot{u}_g(t) \end{bmatrix}. \tag{7}$$

In addition

$$\begin{aligned} \mathbf{M}_{ss} &= \rho_s \int_{V_s} \mathbf{N}_s^T \mathbf{N}_s dV, \\ \mathbf{M}_{ww} &= \frac{\rho_w}{C_w^2} \int_{V_w} \mathbf{N}_w^T \mathbf{N}_w dV, \\ \mathbf{K}_{ss} &= \rho_s \int_{V_s} \mathbf{N}_s^T \mathbf{D}_s^T \mathbf{N}_s dV, \\ \mathbf{K}_{ww} &= \rho_w \int_{V_w} \mathbf{B}_w^T \mathbf{B}_w dV, \\ \mathbf{C}_{sw} &= \mathbf{C}_{ws}^T = -\rho_w \int_{V_w} \mathbf{N}_s^T \mathbf{n} \mathbf{N}_w dS, \\ \mathbf{C}_{ss} &= \alpha \mathbf{M}_{ss} + \beta \mathbf{K}_{ss}, \end{aligned} \tag{8}$$

where $\mathbf{N}_s$ and $\mathbf{N}_w$ are standard isoparametric shape function matrices for shell and fluid elements, respectively. ρ_s and V_s are the density and volume of the tank, $\mathbf{D}_s$ is the elastic matrix of shell elements, $\mathbf{M}_{ss}$ and $\mathbf{K}_{ss}$ are the mass and stiffness matrices for the tank, and $\mathbf{M}_{ww}$ and $\mathbf{K}_{ww}$ are the mass and stiffness matrices for water. 1 is the column vector which has the same dimension of nodal relative displacement $\mathbf{U}$, $\mathbf{C}_{ws}$ and $\mathbf{C}_{sw}$ account for FSI between water and tank, and $\mathbf{C}_{ss}$ is the Rayleigh damping matrix for structure, in which α and β are the Rayleigh damping coefficients. As one classical damping matrix, Rayleigh damping matrix can be used for common structures whose components have similar damping mechanism. The damping coefficients α, β and the matrix $\mathbf{B}_w$ in (5) are given by

$$\begin{aligned} \alpha &= \frac{2\zeta\omega_i\omega_j}{\omega_i + \omega_j}, \\ \beta &= \frac{2\zeta}{\omega_i + \omega_j} \\ \mathbf{B}_w &= \begin{bmatrix} \dfrac{\partial N_w^{(1)}}{\partial x} & \dfrac{\partial N_w^{(2)}}{\partial x} & \cdots & \dfrac{\partial N_w^{(n)}}{\partial x} \\ \dfrac{\partial N_w^{(1)}}{\partial y} & \dfrac{\partial N_w^{(2)}}{\partial y} & \cdots & \dfrac{\partial N_w^{(n)}}{\partial y} \end{bmatrix}, \end{aligned} \tag{9}$$

where ζ is the damping ratio of structure, ω_i and ω_j are the frequencies of structure, and n is the number of nodes per fluid element. The chosen frequencies ω_i and ω_j should cover the frequency bands which are concerned in the structural analysis. Moreover, the frequency bands should be considered by the dynamic characteristics of structure and the external loads.

The experimental model is established and analyzed by ADINA software. Solid finite elements are used to simulate the model base and the water tank, and shell finite elements are used to simulate the toughened glass. The software implements the $\phi - u$ described previously and the hydrodynamic pressures can be coupled to the vibration of solid elements by using PBFE. So PBFE are used to simulate water in the tank. The material parameters are the same with experiment shown in Table 1. The numerical model is shown in Figure 9 and the size of mesh is about 20–30 mm.

3.2. Modal Analysis and Comparison. Considering the symmetry of structure, the repeated modes are ignored. The first four sloshing frequencies and the sloshing modes are shown in Figure 10. The frequencies are compared with the experimental results and the errors are listed in Table 5. The errors of 1st, 2nd, and 4th sloshing frequencies are all less than 1%. Although the error of 3rd sloshing frequency is larger than other three, 6.15% error is acceptable. Through the comparison, the reasonableness of numerical analysis and the accuracy of experimental results are verified.

3.3. Time History Analysis and Comparison. In this part, the reasonableness of numerical analysis is verified in time history analysis. The three-direction acceleration time histories are used as inputs at the foundation of model and the time history curves are shown in Figure 5(b). The durations of inputs are 6.142 s and the duration of strong motion is about 3.50 s. Considering the free sloshing of water, the calculation time is extended to 10 s.

Under the three-direction seismic loadings, the water is rotating along the walls of tank. The numerical results of vertical sloshing displacement are shown in Figure 11. It can be seen that the maximum vertical displacement appears not only in x-axis or y-axis but also in other directions shown in Figure 11(a). The reason is that the rotating phenomenon of liquid surface often appears under seismic loadings and

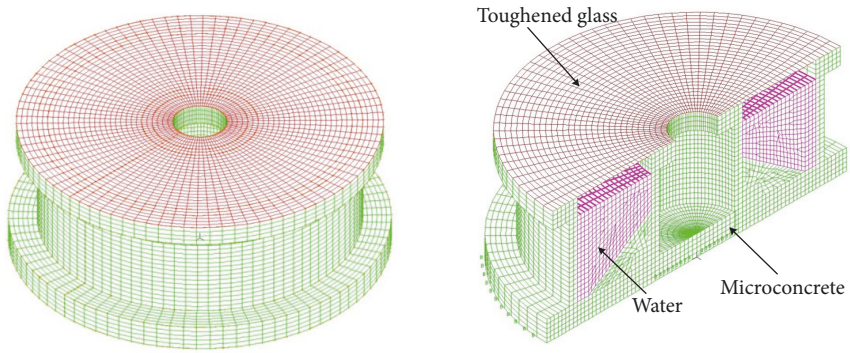

Figure 9: Numerical model of water tank. (a) 3-D view. (b) Cross section.

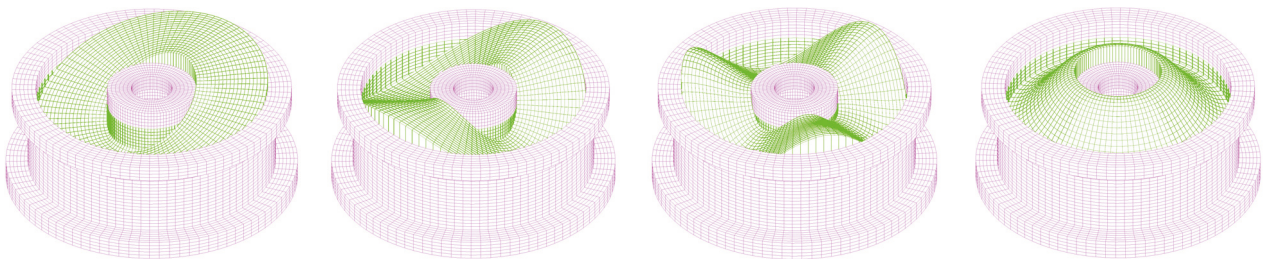

Figure 10: First four sloshing modes. (a) 1st sloshing frequency 0.4926 Hz. (b) 2nd sloshing frequency 0.8399 Hz. (c) 3rd sloshing frequency 1.0631 Hz. (d) 4th sloshing frequency 1.2085 Hz.

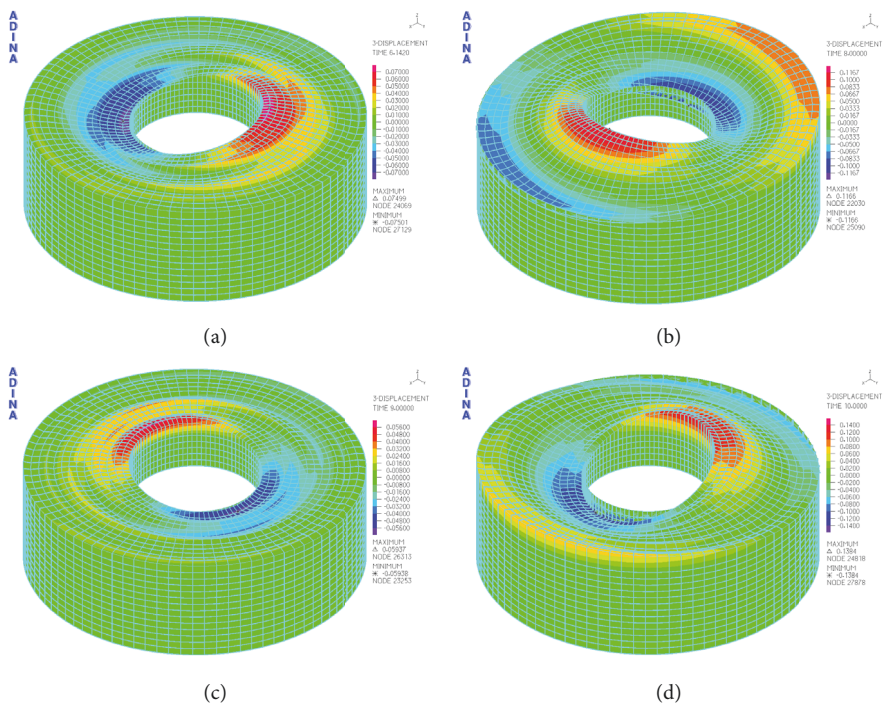

Figure 11: Numerical results of vertical sloshing displacement. (a) Vertical sloshing displacement at 6.142 s. (b) Vertical sloshing displacement at 8.000 s. (c) Vertical sloshing displacement at 9.000 s. (d) Vertical sloshing displacement at 10.000 s.

Table 5: First four sloshing frequencies.

Sloshing modes	Average value (Hz)	Numerical analysis (Hz)	Errors (%)
1	0.4938	0.4926	−0.24
2	0.8404	0.8399	−0.06
3	1.0015	1.0631	+6.15
4	1.2188	1.2085	−0.85

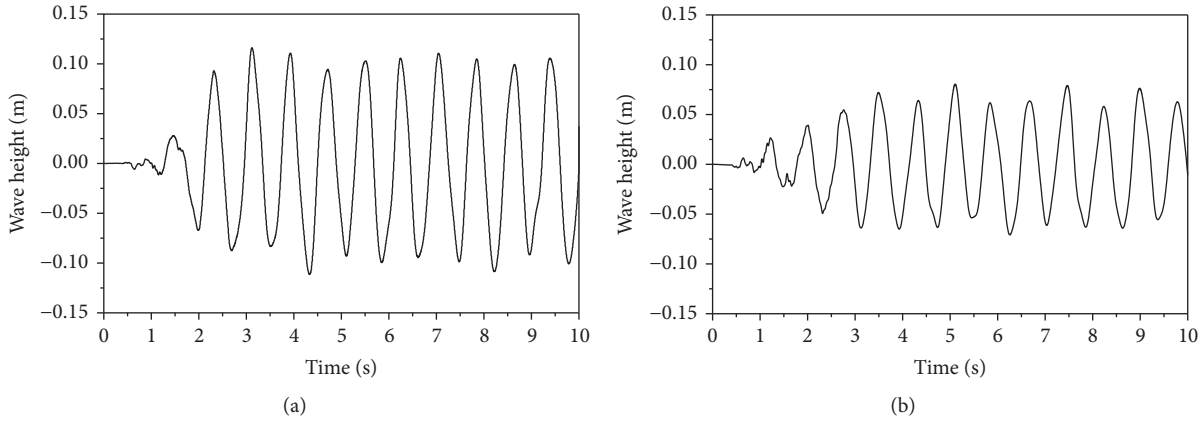

Figure 12: The wave height under three-direction seismic loadings. (a) Inner wall-X section. (b) Outer wall-X section.

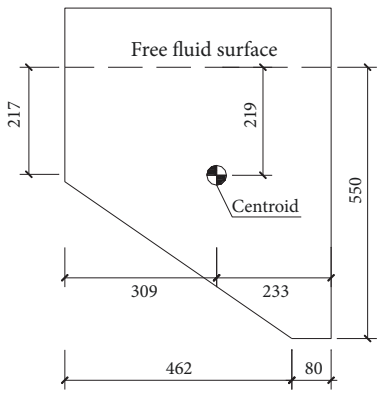

Figure 13: The location of centroid of fluid (unit: mm).

the rotation direction is random. This is a typical bifurcation phenomenon of liquid in three-dimensional space and the occurrence condition is related to external excitation and the viscosity of liquid [26].

The wave height time histories at the inner wall and the outer wall in x cross section are shown in Figure 12. It can be seen that the vertical displacement of fluid surface at the inner wall is larger than that at the outer wall. After the seismic loadings, the sloshing of water is continuous and attenuated constantly.

It is known that the sloshing wave height is related to many factors such as the density of liquid, the depth of liquid, and the shape of tank. The liquid properties are determined in this paper, so the depth of liquid and the shape of tank may influence the wave height. As shown in Figure 13, the cross section of water tank is irregular. The liquid depth near the inner wall is about forty percent of the liquid depth near the outer wall and the centroid of liquid is closer to the outer wall. So the sloshing near the inner wall is more obvious than outer wall.

Under seismic loadings, the liquid in the containers will slosh and impact the walls of tank to affect the structural response. The hydrodynamic pressure occurs because of the liquid motion and it may influence the structural intensity of water tank. The stronger the influence is, the higher the hydrodynamic pressure is and the larger the variation of wave elevation is. The structural response of water tank will directly affect the response of the nuclear island building. So the hydrodynamic pressure should be considered in the dynamic analysis of water tank. The hydrodynamic pressure results of numerical model are compared with those of the experiment. Four reference points at the outer wall, inner wall, and bottom are chosen for comparison and the results are shown in Figure 14. The locations of PWPS are shown in Figure 4.

Figure 14(a) shows the hydrodynamic pressure time history of No. 8 PWPS. The shapes of two curves are in good agreement generally. At the duration of seismic loadings (0–6.142 s), the curve of simulation has the smaller peaks than experimental one. In the stage of free sloshing, the peaks of two curves are close. But the corresponding times of peaks are not the same and have some deviations.

Figure 14(b) shows the hydrodynamic pressure time history of No. 9 PWPS. The simulation data agree well with the experimental results in the shape of curve and the peaks. However, the experimental results are larger obviously at certain time points.

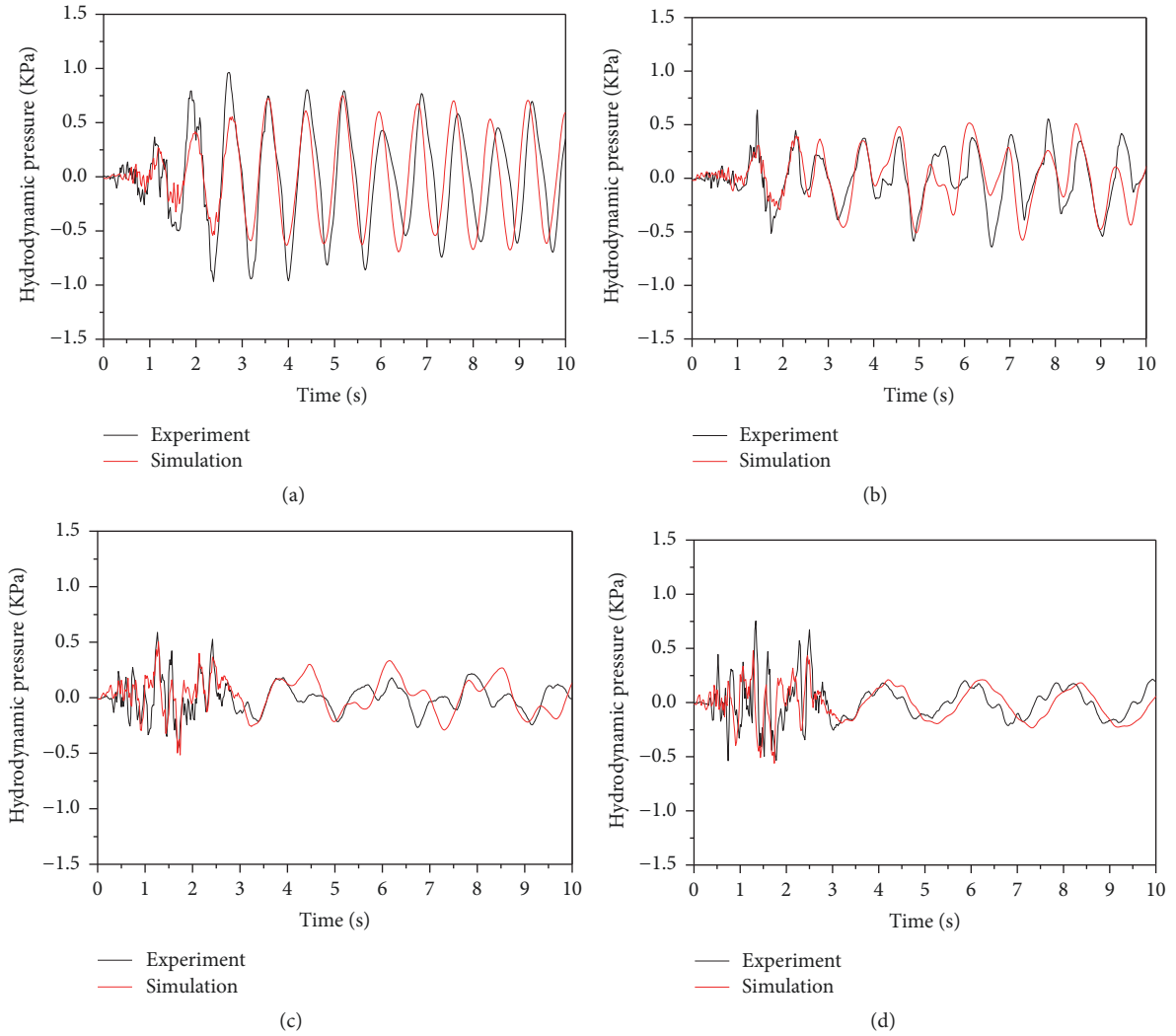

FIGURE 14: The hydrodynamic pressure under three-direction seismic loadings. (a) No. 8 PWPS. (b) No. 9 PWPS. (c) No. 10 PWPS. (d) No. 12 PWPS.

Figure 14(c) shows the hydrodynamic pressure time history of No. 10 PWPS. The two curves do not have good agreement, especially after the strong motion. But the peaks of two curves are close in the first 3 s.

Figure 14(d) shows the hydrodynamic pressure time history of No. 12 PWPS. The trends of two curves are similar to Figure 14(a). The curve of simulation has the smaller peaks in the duration of strong motion. Moreover, the peaks of two curves are close after 3.5 s.

The four PWPS are located at outer wall, inner wall, the bottom, and the junction of wall and bottom separately. So the comparison results can verify the reasonableness of numerical analysis. The simulation data in Figures 14(a), 14(b), and 14(d) agree with the experimental results in general. No. 8 and No. 9 PWPS are close to the free liquid surface, and No. 12 PWPS is at the middle of inclined bottom. So the sloshing response of the three reference points is simple and the curves agree well. But it is also found that the simulation data of No. 10 PWPS fit poorly with experimental results.

It is well known that centroid vibration is the main source of sloshing force and moment. The centroid of liquid in the tank is shown in Figure 13. It can be seen that the location of centroid in vertical direction is very close to No. 10 PWPS. The centroid moves near the initial position when the external excitation is applied, especially in the horizontal direction. Moreover, No. 10 PWPS is at the junction of wall and bottom. These factors may make the sloshing response complicated at No. 10 PWPS. The numerical analysis could not simulate the complex sloshing well during the whole process, but the peak and the trough of two curves do not have too much difference in Figure 14(c).

In general, the accuracy of the formulation of PBFE is acceptable. It can be used to simulate the seismic response of nuclear island building considering the FSI effect and study on the influence of FSI on the seismic response.

4. Conclusion

A 1/16 scaled model was designed and the shaking table test was done in this study. PWPS and cameras were used to record the time histories of hydrodynamic pressure and the attenuation data of wave height. Based on the test data, the sloshing frequencies were recognized by FFT of hydrodynamic pressure time histories and 1st sloshing damping ratio was calculated using logarithmic decrement method. A numerical model of experimental water tank was established by ADINA software. Then modal analysis and time history analysis were done and the numerical results were compared with experimental data. The following conclusions could be got. They can be used to analyze the FSI of nuclear island building and simplify the sloshing analysis.

(1) The measuring method of the water responses mentioned in this paper can be used to recognize sloshing frequencies. Comparing with the numerical analysis, the result is acceptable.

(2) 1st sloshing damping ratio of PCS water tank is 0.5138% and the suggestion in the specification can be used for this irregular annular cylindrical water tank. But more studies will be done to verify whether this conclusion is suitable for other shape tanks.

(3) The formulation of PBFE is suitable for modal analysis and time history analysis, and the accuracy of numerical results is acceptable.

Indeed, this paper focuses on the experimental model of PCS water tank and the verification of numerical method. For the real nuclear island building, water tank and FSI effect may influence the seismic response, floor response spectra, and the bearing capacity of the structure. Thus more studies should be done aimed at the seismic response of the whole nuclear island building.

Conflicts of Interest

There are no conflicts of interest related to this paper.

Acknowledgments

This research is supported by the National Natural Science Foundation of China (51738001, 51421005). Thanks are due to the 19th International Conference on Structural Engineering, Vibration and Aerospace Engineering.

References

[1] T. L. Schulz, "Westinghouse AP1000 advanced passive plant," *Nuclear Engineering and Design*, vol. 236, no. 14–16, pp. 1547–1557, 2006.

[2] R. A. Ibrahim, *Liquid Sloshing Dynamics*, Cambridge University Press, 2005.

[3] F. Axisa and J. Antunes, *Modelling of Mechanical System: Fluid-Structure Interaction*, vol. 3, Butterworth-Heinemann, Oxford, UK, 2009.

[4] R. Lo Frano, "Evaluation of the fluid-structure interaction effects in a lead-cooled fast reactor," *Nuclear Technology*, vol. 33, no. 1, pp. 491–499, 2015.

[5] O. M. Faltinsen, O. F. Rognebakke, I. . Lukovsky, and A. N. Timokha, "Multidimensional modal analysis of nonlinear sloshing in a rectangular tank with finite water depth," *Journal of Fluid Mechanics*, vol. 407, pp. 201–234, 2000.

[6] O. M. Faltinsen, O. F. Rognebakke, and A. N. Timokha, "Resonant three-dimensional nonlinear sloshing in a square-base basin analysis of nonlinear sloshing in a rectangular tank," *Journal of Fluid Mechanics*, vol. 487, pp. 1–42, 2003.

[7] R. Lo Frano and G. Forasassi, "Conceptual evaluation of fluid-structure interaction effects coupled to a seismic event in an innovative liquid metal nuclear reactor," *Nuclear Engineering and Design*, vol. 239, no. 11, pp. 2333–2342, 2009.

[8] R. Lo Frano and G. Forasassi, "Preliminary evaluation of seismic isolation effects in a generation IV reactor," *Energy*, vol. 36, no. 4, pp. 2278–2284, 2011.

[9] R. Lo Frano and G. Forasassi, "Preliminary evaluation of structural response of ELSY reactor in the after shutdown condition," *Nuclear Engineering and Design*, vol. 246, pp. 298–305, 2012.

[10] C. Zhao, J. Chen, and Q. Xu, "Dynamic analysis of AP1000 shield building for various elevations and shapes of air intakes considering FSI effects subjected to seismic loading," *Progress in Nuclear Energy*, vol. 74, pp. 44–52, 2014.

[11] Q. Xu, J. Chen, C. Zhang, J. Li, and C. Zhao, "Dynamic analysis of AP1000 shield building considering fluid and structure interaction effects," *Nuclear Engineering and Technology*, vol. 48, no. 1, pp. 246–258, 2016.

[12] D. Lu, Y. Liu, and X. Zeng, "Experimental and numerical study of dynamic response of elevated water tank of AP1000 PCCWST considering FSI effect," *Annals of Nuclear Energy*, vol. 81, pp. 73–83, 2015.

[13] Y. Liu, D. Lu, J. Dang, S. Wang, and X. Zeng, "Equivalent mechanical model for structural dynamic analysis of elevated tank like AP1000 PCCWST," *Annals of Nuclear Energy*, vol. 85, pp. 1175–1183, 2015.

[14] H. Takahara and K. Kimura, "Frequency response of sloshing in an annular cylindrical tank subjected to pitching excitation," *Journal of Sound and Vibration*, vol. 331, no. 13, pp. 3199–3212, 2012.

[15] G. W. Housner, "Dynamic pressure on accelerated fluid containers," *Bulletin of the seismological society of American*, vol. 44, pp. 15–35, 1957.

[16] G. W. Housner, "The dynamic behavior of water tanks," *Bulletin of the Seismological Society of America*, vol. 53, no. 2, pp. 381–387, 1963.

[17] D. D. Kana, "Status and research needs for prediction of seismic response in liquid containers," *Nuclear Engineering and Design*, vol. 69, no. 2, pp. 205–221, 1982.

[18] "American society of civil engineers. Seismic analysis of safety-related nuclear structures and commentary. ASCE 4-98".

[19] "ACI 350.3-06. Seismic design of liquid-containing concrete structures and commentary. American Concrete Institute".

[20] C. G. Lin and Z. S. Yu, *An advanced passive plant AP1000*, Atomic Energy Press, 2008.

[21] A. K. Chopra, *Dynamics of Structures: Theory and Applications to Earthquake Engineering*, vol. 4th, Prentice Hall, 2012.

[22] ADINA R&D, "Theory and modeling guide," Rep. ARD 10-7, Watertown, MA, 2010.

[23] K. Wei, W. Yuan, and N. Bouaanani, "Experimental and numerical assessment of the three-dimensional modal dynamic response of bridge pile foundations submerged in water," *Journal of Bridge Engineering*, vol. 18, no. 10, pp. 1032–1041, 2013.

[24] N. Bouaanani and F. Y. Lu, "Assessment of potential-based fluid finite elements for seismic analysis of dam-reservoir systems," *Computers & Structures*, vol. 87, no. 3-4, pp. 206–224, 2009.

[25] L. G. Olson and K.-J. Bathe, "Analysis of fluid-structure interactions. a direct symmetric coupled formulation based on the fluid velocity potential," *Computers & Structures*, vol. 21, no. 1-2, pp. 21–32, 1985.

[26] H. N. Abramson, W. H. Chu, and D. D. Kana, "Some studies of nonlinear lateral sloshing in rigid containers," *Journal of Applied Mechanics*, vol. 33, no. 4, pp. 777–784, 1964.